

Zonal Modes of Cosmic Microwave Background Temperature Maps

Jo Short* and Peter Coles

School of Physics and Astronomy, Cardiff University, Queens Buildings, 5 The Parade, Cardiff, CF24 3AA, United Kingdom.

2 November 2018

ABSTRACT

All-sky maps of the cosmic microwave background temperature fluctuations are usually represented by a spherical harmonic decomposition, involving modes labeled by their degree l and order m (where $-l \leq m \leq +l$). The *zonal modes* (i.e those with $m = 0$) are of particular interest because they vary only with galactic latitude; any anomalous behavior in them might therefore be an indication of erroneous foreground subtraction. We perform a simple statistical analysis of the modes with low l for sky maps derived via different cleaning procedures from the Wilkinson Microwave Anisotropy Probe (WMAP), and show that the zonal modes provide a useful diagnostic of possible systematics.

Key words: cosmology: cosmic microwave background — cosmology: observations — methods: data analysis

1 INTRODUCTION

Observations of the temperature anisotropies of the cosmic microwave background (CMB), particularly those from the Wilkinson Microwave Anisotropy Probe (WMAP) (Bennett et al. 2003; Hinshaw et al. 2009), form the foundations of the remarkably successful “concordance” cosmological model (Coles 2005). An essential ingredient of this model is the assumption that the primordial density fluctuations that seeded the formation of galaxies and large-scale structure were statistically homogeneous and Gaussian. Versions of the inflation scenario based on the idea of a single slow-rolling scalar field predict levels of non-Gaussianity too small to be observed. On the other hand, multi-field inflation models, and models with a non-standard kinetic term for the inflaton, may yield larger non-Gaussian effects which could in principle be detected in current or next-generation observations (Bartolo et al. 2002; Bernardeau & Uzan 2002; Lyth et al. 2003; Dvali et al. 2004; Arkani-Hamed et al. 2004; Alishahiha et al. 2004; Bartolo et al. 2004; Chen et al. 2007; Battfeld & Battfeld 2007; Koyama et al. 2007). Analysis of currently available WMAP data provide strong limits on the level of non-Gaussianity (Komatsu et al. 2003; Spergel et al. 2007; Creminelli et al. 2007; Hikage et al. 2008). On the other hand, Yadav & Wandelt (2008) recently reported a detection of primordial non-Gaussianity at greater than 99.5% significance. Further detailed analyses of non-Gaussianity

are clearly necessary in order to reconcile and understand the various constraints and claimed detections.

The greatest barrier to the detection of non-Gaussianity, or other departures from the framework of the concordance cosmological model, is the presence of residual foreground contamination or other systematic errors. Since our own Galaxy emits at microwave frequencies, the emission from local foregrounds must be carefully cleaned before a map can be obtained that is suitable for analysis. One way of avoiding this problem is to cut out regions near the Galactic plane where contamination is particularly severe, but this throws away the advantage of having full coverage. It is therefore important to produce maps that are as clean as possible over the whole sky for many purposes. However, such cleaning is inevitably approximate and biases are bound to occur (Eriksen et al. 2005; Naselsky, Verkhodanov & Nielsen 2008; Chiang, Naselsky & Coles 2009). Circumstantial evidence exists that may be interpreted as being due to the presence of residual Galactic foregrounds in the WMAP data, or some other artefact of the cleaning process (Chiang, Naselsky & Coles 2007; Chiang et al. 2007), but in the absence of a more complete characterization of the galactic emission the situation remains unclear.

In this *Article* we propose and test a simple diagnostic analysis that offers the possibility of identifying foreground-related biases and systematics in all-sky maps of the CMB.

* Email: ShortJ1@cardiff.ac.uk (JS); Peter.Coles@astro.cf.ac.uk (PC)

2 ZONAL MODES OF CMB MAPS

The statistical variation of the CMB temperature, $T(\theta, \varphi)$, over the celestial sphere can be conveniently decomposed into spherical harmonic modes:

$$T(\theta, \varphi) = \sum_{\ell=0}^{\infty} \sum_{m=-\ell}^{\ell} a_{\ell m} Y_{\ell m}(\theta, \varphi), \quad (1)$$

where the $Y_{\ell m}(\theta, \varphi)$ are spherical harmonic functions, defined in terms of the Legendre polynomials, $P_{\ell m}$, using

$$Y_{\ell m}(\theta, \varphi) = (-1)^m \sqrt{\frac{(2\ell+1)(\ell-m)!}{4\pi(\ell+m)!}} P_{\ell m}(\cos\theta) e^{im\varphi}, \quad (2)$$

and the $a_{\ell m}$ are complex coefficients which can be expressed with $a_{\ell m} = |a_{\ell m}| \exp(i\Phi_{\ell m})$ where $\Phi_{\ell m}$ are the phases (Coles et al. 2004; Chiang, Naselsky & Coles 2004, 2007, 2009; Stannard & Coles 2005). We have adopted the Condon-Shortly phase definition in the spherical harmonic decomposition.

The spherical harmonics functions, $Y_{\ell m}$, can be visualized by considering their *nodal lines*, i.e. the set of points (θ, φ) on the sphere where the spherical harmonics vanish, i.e. where $Y_{\ell m}(\theta, \varphi) = 0$. Nodal lines are circles, which are either in the latitude or longitude direction with respect to the coordinate system being used; in the case of CMB maps this is usually the galactic coordinate system. The number of nodal lines of each type is determined by the number of zeros of $Y_{\ell m}$ in the latitudinal and longitudinal directions independently. The associated Legendre functions $P_{\ell m}$ possess $\ell - |m|$ zeros in the latitude direction, whereas the trigonometric sin and cos functions possess $2|m|$ zeros in the longitude direction. Two specific orders m are of particular interest at a given ℓ in the context of this work: these denote the *zonal* modes, with $m = 0$, and the *sectoral* modes, with $m = \ell$. In the former case there are no zero-crossings in the longitude direction, so contours of equal temperature run parallel to latitude lines; in the latter the contours run parallel to longitude lines. Examples are shown in Figure 1. In the intermediate cases with $0 < m < \ell$ there are zero-crossings in both directions, giving rise to a patchwork appearance; these are usually called *tesseral* modes.

Statistically isotropic Gaussian random CMB temperature fluctuations on a sphere, of the type that result from the simplest versions of the inflationary paradigm, possess spherical harmonic coefficients ($a_{\ell m}$) whose real and imaginary parts are mutually independent and both Gaussian (Bond & Efstathiou 1987; Coles et al. 2004). The statistical properties of the fluctuations are then completely specified by the angular power spectrum, C_{ℓ} , where

$$\langle a_{\ell m} a_{\ell' m'}^* \rangle = C_{\ell} \delta_{\ell\ell'} \delta_{mm'}. \quad (3)$$

Since T is always real, the complex vectors of the $a_{\ell m}$ on the Argand plane for $m < 0$ are mirror images of those with $m > 0$ with respect to x axis for even m , and with respect to y axis for odd m . Writing

$$a_{\ell m} = x_{\ell m} + iy_{\ell m}, \quad (4)$$

we note that the variances of the real and imaginary parts of $a_{\ell m}$ for $m > 0$ are equal

$$\sigma^2(x_{\ell m}) = \sigma^2(y_{\ell m}) \equiv \sigma_{\ell}^2 = \frac{1}{2}C_{\ell}, \quad (5)$$

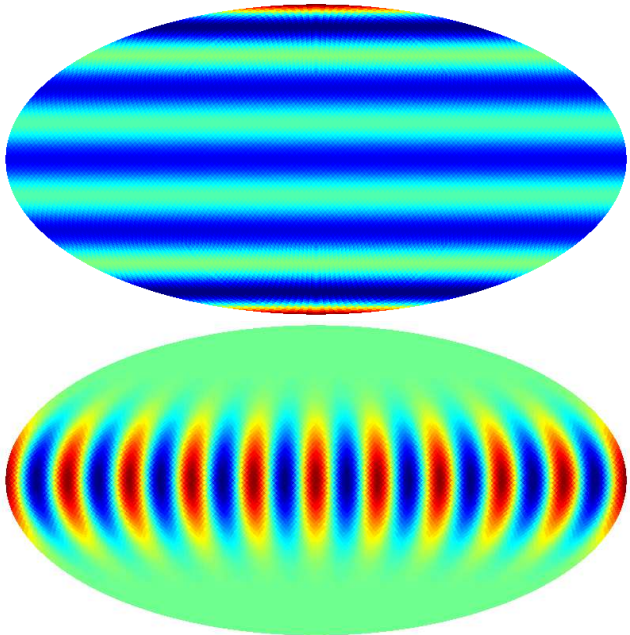


Figure 1. Illustrative examples of zonal and sectoral modes for $l = 10$; the first example is the zonal mode with $m = 0$ and the second is the sectoral mode with $m = 10$.

which depends only on ℓ . The distributions of $x_{\ell m}$ and $y_{\ell m}$ are independent Gaussians with these variances and zero mean. The amplitudes $|a_{\ell m}|$ for these modes therefore have a Rayleigh distribution with random phases (Bond & Efstathiou 1987; Stannard & Coles 2005). For $m = 0$, the imaginary part of $a_{\ell m}$ must be zero, so this mode always has zero phase $\Phi_{\ell m}$. This is because the phase relates to the variation around the polar axis only. However, the distribution $x_{\ell m}$ for $m = 0$ should be equal to that of the other real parts at a given ℓ , namely a Gaussian with zero mean and stated variance.

3 STATISTICAL ANALYSIS

3.1 Preamble

Statistical analysis of the spherical harmonics of CMB maps usually involves using all modes in an equivalent manner. However, since the zonal modes in particular have such a special relationship to the galactic coordinate system, it is worth looking at their properties independently to see whether they hold any clues to possible residual contamination aligned with the Galactic plane.

In order to construct a test which involved the smallest possible number of assumptions, and in particular avoided the need to make estimates of the power-spectrum C_{ℓ} along the way, we focused on the modes with maximum or minimum amplitude at a given ℓ . If all modes are statistically equivalent then the different orders m at a given ℓ are equally likely to furnish the maximum (or minimum) amplitude $|a_{\ell m}|$. A preference for modes with $m = 0$ to display the maximum (or minimum) amplitude might therefore be plausibly interpreted as evidence that the zonal modes are either contaminated with residual foreground, or that foregrounds have been excessively subtracted. Both of these possibilities

are supported by other evidence (Chiang, Naselsky & Coles 2009; Chiang et al. 2007; Naselsky, Verkhodanov & Nielsen 2008).

3.2 Data

The maps analyzed in this paper are the 1-year (Bennett et al. 2003), 3-year (Jarosik et al. 2007), and 5-year (Hinshaw et al. 2009) Internal Linear Combination (ILC) maps from the WMAP team, the 1 and 3 year maps from Tegmark et al. (2003) and the harmonic ILC map by Kim et al. (2008) (hereafter ILC1, ILC3, ILC5, TOH1, TOH3 and HILC). We apply three tests to these maps, which are described in detail below.

3.3 Extremal Mode Counts

For our first test, we analyze the value of m associated with the largest (or smallest) amplitude $|a_{lm}|$ for a given l in the ranges $[0, 10]$ and $[0, 20]$. Since the a_{lm} for all orders m at a given l should have the same variance in the null hypothesis (of a stationary Gaussian random field), the minimum or maximum value of $|a_{lm}|$ should not occur preferentially at any particular value of m . We use a very straightforward method to establish whether this is the case. For each map we simply count the number of occurrences (i.e. numbers of separate degrees l within the range analyzed) for which the minimum or maximum value amplitude occurs at $m = 0$ (the zonal mode) or $m = l$ (the sectoral mode). These counts are recorded in Table 1. What we have done is to identify, at each degree l , the value of m which has the minimum (or maximum) value of $|a_{lm}|$. If the minimum is at $m = 0$ then this contributes to the count in Column 3 of the table; if the maximum is $m = 0$ it contributes to the count in Column 4; likewise occurrences of extrema at $m = l$ contribute to the counts in the following two columns. For results where the maximum $l = 10$ the counts are out of a total of 11 and for maximum $l = 20$ they are out of a total of 21.

We have restricted our analysis to low l modes partly to keep the computational cost of the simulations down but mainly because the high l modes are known not to be clean anyway so it would not reveal anything interesting to find zonal or sectoral anomalies among them. We have also given results for the sectoral modes for comparison, but there are no significant anomalies associated with them and we shall not discuss them further in this paper.

3.4 Significance Levels

It is not a trivial matter to calculate significance levels analytically for this test because the number of available orders m increases with l . It is obviously much more probable that the minimum amplitude is at $m = 0$ for $l = 2$ than for $l = 20$ under the null hypothesis. Assessing the significance of the number of occurrences of zonal or sectoral extrema involves a messy exercise in combinatorics. However, we can finesse this difficulty by instead comparing the actual maps with simulations constructed according to the Gaussian assumption described in Section 2.

It is also possible that the cleaning process used to remove foreground contamination from the raw observations

Map	l_{\max}	$m_{\min} = 0$	$m_{\max} = 0$	$m_{\min} = l$	$m_{\max} = l$
ILC1	10	6	3	3	4
ILC3	10	7	2	2	4
ILC5	10	7	2	2	4
TOH1	10	6	2	3	4
TOH3	10	8	2	2	4
HILC	10	8	2	1	5
ILC1	20	9	3	3	6
ILC3	20	9	2	2	5
ILC5	20	8	2	2	4
TOH1	20	8	3	3	5
TOH3	20	11	2	2	5
HILC	20	10	2	1	6

Table 1. This table shows, for the various cleaned all-sky maps described in the text, the maximum value of the degree l considered, and, in the following four columns, the number of times (i.e. number of values of l) for which the minimum (or maximum) amplitude a_{lm} is at $m = 0$ (zonal mode) or $m = l$ (sectoral mode). For example, the $m_{\min} = 0$ and $\max l = 20$ result for TOH3 means that 11 out of 21 different values of the degree $l \in [0, 20]$ have the lowest value of the amplitude $|a_{lm}|$ at $m = 0$.

might in any case introduce some sort of bias into the statistical distribution of amplitudes or induce correlations between different modes. To circumvent this difficulty, as well as the one noted in the previous paragraph, we therefore base the confidence levels on our test on a set of simulations performed by Eriksen et al. (2005), which takes “raw” sky maps, generated assuming Gaussian fluctuations, adds simulated foregrounds and then recovers the signal using the ILC methodology. The simulated maps we use therefore already take into account any “artificial” correlations that the ILC process may generate. These are particularly useful as they allow us to assess whether any anomalies we do actually find must be above the level known to be introduced by the ILC cleaning process.

In order to calculate significance levels of the results in Table 1 we used an ensemble of $N = 10000$ independent Monte Carlo realizations of Gaussian skies, contaminated with foreground and then cleaned according to the ILC prescription as described above. We use these simulations to construct empirical distributions of the count statistics displayed in the previous table and from these we compute the empirical significance levels shown in Table 2.

The corresponding probabilities of the results in Table 2 were calculated using the Monte Carlo simulations detailed above by counting the number of occurrences of each configuration shown in Table 1. Note that since we are using $N = 10000$ independent simulations we expect the results to be affected by Poisson fluctuations at the level of order \sqrt{N} , which means we expect the probabilities in Table 2 only to be accurate to about 1% or so.

For the case of zonal maxima, it is clear that there no significant results above 2σ (i.e. the 95% level), but the zonal minima do show a significant result in the TOH3 and HILC maps for $l < 10$. It is also interesting to note that the TOH3 map gives a higher significance level than the TOH1 map, as does the ILC5 map compared to the corresponding 1 yr map ILC1.

It is worth stressing that each column represents a single

Map	l_{\max}	$m_{\min} = 0$	$m_{\max} = 0$	$m_{\min} = l$	$m_{\max} = l$
ILC1	10	75.2	15.4	64.2	80.4
ILC3	10	91.7	0.0	25.5	80.4
ILC5	10	91.7	0.0	25.5	80.4
TOH1	10	75.2	0.0	64.2	80.4
TOH3	10	98.2	0.0	25.5	80.4
HILC	10	98.2	0.0	0.0	94.9
<hr/>					
ILC1	20	88.0	6.3	46.8	92.8
ILC3	20	88.0	0.0	15.6	80.1
ILC5	20	74.1	0.0	15.6	57.1
TOH1	20	74.1	6.3	46.8	80.1
TOH3	20	98.4	0.0	15.6	80.1
HILC	20	95.0	0.0	0.0	92.8

Table 2. Monte Carlo estimates of the probabilities of the extremal mode counts, i.e occurrences of $m_{\text{ext}} = 0$ or l , for the various CMB maps shown in Table 1. These are computed by forming the empirical distribution of the counts over an ensemble of simulated skies and counting what fraction of the ensemble gives the results obtained for the real maps. For example, in the case of the $m_{\min} = 0$ and $\max l = 20$ result for TOH3, we find that, out of 10000 simulations, 9844 have *less than* 11 (from Table 1) occurrences of minimum amplitudes at $m = 0$. Given the probable sampling accuracy of around one percent, we have rounded the results. Note that these are discrete distributions, so the zero percentages do not necessarily indicate cases of exceptional significance, just that it is not possible to have less than the observed number of occurrences. In other words, we should treat this as a one-sided statistical test.

statistical test using all the information contained in the modes with degree l in the range analyzed, and therefore represent genuine *a priori* significance levels. For example, in the case of the $m_{\min} = 0$ and $\max l = 20$ result for TOH3 described in the caption for Table 2, the probability that a genuinely Gaussian CMB sky processed in the way we described above, would produce as many zonal minima as observed is only $(100 - 98.4) = 1.6\%$.

3.5 Mode Variances

We performed a second investigation in order to locate the source of the apparent deficit in the zonal modes. The results above suggest that the amplitudes when $m = 0$ are low compared to simulations, so this test considers whether this is because the variance of the amplitudes is lower for $m = 0$ than for all other m . Since there is no imaginary part to the amplitude when $m = 0$, just the real parts of the a_{lm} (i.e. the x_{lm}) are considered. The variances of the x_{l0} for the ILC5 and TOH3 maps are calculated and the corresponding probabilities are calculated by comparing these values to the variances of the x_{l0} from the simulations. The results in Table 3 provide evidence that the variance of the x_{l0} in the ILC5 and TOH3 maps is significantly smaller than in the simulations. For comparison, the same calculation is also applied ‘for all m ’ and ‘for all m not equal to 0’. The results for all m show that the variance in the TOH3 and ILC5 maps is lower than in the simulations, which is consistent with the previously reported low variance in the combined Q + V + W map by Monteserin et al. (2008). This leads to the further question of whether the zonal mode amplitudes

Map	$m = 0$	$\forall m$	$m \neq 0$
ILC5	97.1	93.2	69.0
TOH3	97.6	93.8	69.2

Table 3. Percentage of simulations, for given m , where the variance of the x_{lm} is greater than the specified map. For example take the TOH3 result for $m=0$. We found that, out of 10000 simulations, 9757 had a variance of the x_{l0} greater than the variance of the x_{l0} in the TOH3 map. Since the Poisson fluctuations are of order 1% we have rounded the resulting percentage.

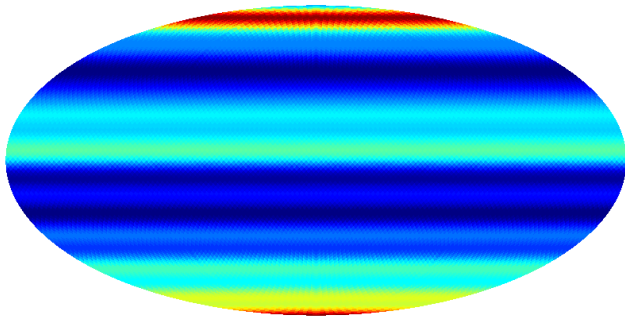


Figure 2. Reconstructed CMB map for WMAP ILC 5 yr map using only the $m = 0$ modes for $l = [0, 20]$ i.e. this map is the WMAP ILC 5 yr map which has had all but the $|a_{l0}|$ set to zero. The colour scale is marked in milliKelvin.

are entirely responsible for this low variance. Table 3 shows that by removing the $m = 0$ amplitudes the number of simulated maps with a variance greater than the test map falls dramatically, suggesting that indeed the low variance of the $m = 0$ amplitudes does have a notable affect on the overall variance of the amplitudes.

3.6 Map Structure

It is interesting to reconstruct what the CMB sky would look like if it only contained the zonal modes, as these are the ones that appear to have anomalous properties; the result in Figure 2 shows that the deepest minima are just below and slightly above the Galactic plane. For our third test we considered whether these minima (and also the maxima of the map) are of abnormal amplitude compared to the simulated maps; this test is done in pixel-space rather than using the a_{lm} . Because the resolution of the maps is quite low, we restricted our analysis to the parts of the map that are well-sampled (i.e. we neglected the Galactic pole areas). Monte Carlo simulations were run to estimate the probability of a maximum or minimum as seen in the map. The resulting probabilities are shown in Table 4. Similarly to Larson & Wandelt (2004), who find that the hot and cold spots of the separate WMAP frequency maps are not hot and cold enough, we find that the maxima (and minima) of the zonal maps are not as high (and low) as expected compared to the simulations. The trend reinforced again in this table seems to be that the anomalous result becomes increasingly significant as the maps supposedly improve.

Map	minimum	maximum
ILC1	73.0	88.1
ILC3	82.1	98.9
ILC5	81.2	99.0
TOH1	77.9	95.0
TOH3	95.2	98.6
HILC	85.4	97.9

Table 4. Probability of the observed maxima and minima in zonal maps, as derived from Monte Carlo simulations. For example take the results for ILC5: out of 10000 simulations, 8124 have a minimum ‘temperature’ in the $m = 0$ only map which is *less than* that observed in the ILC5 $m = 0$ map (see Figure 2). Similarly, out of 10000 simulations, 9902 have a maximum ‘temperature’ in the $m = 0$ map which is *greater than* that observed in the ILC5 $m = 0$ map.

4 DISCUSSION

We have presented a simple statistical analysis based on properties of the zonal modes of cosmic microwave background maps, i.e. those aligned parallel to the Galactic plane. An application of the test to various cleaned CMB maps gives interesting results. At the 95 per cent level, no significant anomalies appear in the WMAP ILC maps (Bennett et al. 2003; Jarosik et al. 2007; Hinshaw et al. 2009) but there seems to be a significant tendency in some other maps (Tegmark et al. 2003; Kim et al. 2008) to have zonal modes with systematically lower amplitudes than would be expected in the concordance model. Intriguingly, the maps that provide the most significant departures from the behavior expected under the null hypothesis are those based on later issues of the WMAP data. We have also showed that the low variance of the maps is more significant where you consider only the zonal amplitudes. This shows that zonal modes have a notable contribution towards this low variance. Finally, we considered the distribution of maxima and minima in zonal maps which again reinforced the earlier finding that the anomalies increase with later data releases. The question of whether this is due to increasing over subtraction, or whether decreasing noise is revealing an underlying anomaly such as a systematic problem, cannot be distinguished with current data.

Of course the maps themselves are not statistically independent. Indeed, if the cleaning processes involved were perfect then they would all be identical. The different results we have found for the different maps are attributable to the nature of the zonal modes and their extra sensitivity to the structures associated with the Galactic Plane. The appearance of significant anomalies in some maps rather than others is not a statistical fluke but is clear evidence that some cleaning methods leave artifacts in the distribution of mode amplitudes.

It must be noted that the probabilities we quote of around 98 to 99 percent are not overwhelming, so the results we have obtained are indicative rather than decisive. This is not surprising, given the relatively small number of modes we used. However, we repeated the analysis for a coordinate system aligned with the Ecliptic, rather than Galactic plane, and found no significant results at all. This lends further credence to our interpretation of the out-

come of our analysis in terms of an effect related to over-subtraction of Galactic emission (Chiang, Naselsky & Coles 2009; Naselsky, Verkhodanov & Nielsen 2008), which becomes increasingly pronounced with each data release. A more definitive result will have to wait until more detailed foreground subtraction can be attempted, such as will be the case with the *Planck* satellite.

ACKNOWLEDGMENTS

Jo Short receives support from a Science & Technology Facilities Council (STFC) doctoral training grant. We would like to thank Pavel Naselsky for interesting discussions. We gratefully acknowledge the use of the HEALPIX package (Górski et al. 2005).

REFERENCES

- Alishahiha M., Silverstein E., Tong D., 2004, Phys. Rev. D., 70, 123505
- Arkani-Hamed N., Creminelli P., Mukohyama S., Zaldarriaga M., 2004, JCAP, 4, 1
- Bartolo N., Matarrese S., Riotto A., 2002, Phys. Rev. D., 65, 103505
- Bartolo N., Komatsu E., Matarrese S., Riotto A., 2004, Phys. Rept., 402, 103
- Battefeld D., Battefeld T., 2007, JCAP, 5, 12
- Bennett C. L. et al., 2003, ApJS, 148, 1
- Bernardeau F., Uzan J.-P., 2002, Phys. Rev. D., 66, 103506
- Bond J. R., Efstathiou G., 1987, MNRAS, 226, 655
- Chen X., Easther R., Lim E. A., 2007, JCAP, 6, 23
- Chiang L.-Y., Naselsky P. D., Coles P., 2004, ApJ, 602, L1
- Chiang L.-Y., Naselsky P. D., Coles P., 2007, ApJ, 664, 8
- Chiang L.-Y., Naselsky P. D., Coles P., 2009, ApJ, 694, 339
- Chiang L.-Y., Coles P., Naselsky P. D., Olesen P., 2007, JCAP, 1, 21
- Coles P., 2005, Nat, 433, 248
- Coles P., Dineen P., Earl J., Wright D., 2004, MNRAS, 350, 989
- Creminelli P., Senatore L., Zaldarriaga M., & Tegmark M., 2007, JCAP, 3, 5
- Dvali G., Gruzinov A., Zaldarriaga M., 2004, Phys. Rev. D., 69, 083505
- Eriksen H. K. et al., 2005, astro-ph/0508196
- Górski K. M., Hivon E., Banday A. J., Wandelt B. D., Hansen F. K., Reinecke E. M., Bartelmann M., 2005, ApJ, 622, 759
- Hikage C., Matsubara T., Coles P., Liguori M., Hansen H. K., Matarrese S., 2008, MNRAS, 389, 1439
- Hinshaw G. et al., 2009, ApJS, 180, 225
- Jarosik N. et al., 2007, ApJS, 170, 263
- Kim J. et al., 2008, Phys. Rev. D, 77, 103002
- Komatsu E. et al., 2003, ApJS, 148, 119
- Koyama K., Mizuno S., Vernizzi F., Wands D., 2007, JCAP, 11, 24
- Larson D. L., Wandelt B. D., 2004, ApJ, 613, L85-88
- Lyth D. H., Ungarelli C., Wands D., 2003, Phys. Rev. D., 67, 023503
- Monteserin C. et al., 2008, MNRAS, 387, 209

6 *Short & Coles*

- Naselsky P. D., Verkhodanov O. V., Nielsen M. T. B., 2008, *AstBu*, 63, 216
- Spergel D. N. et al., 2007, *ApJS*, 170, 377
- Stannard A., Coles P., 2005, *MNRAS*, 364, 929
- Tegmark M. et al., 2003, *Phys. Rev. D*, 68, 123523
- Yadav A. P. S., Wandelt B. D., 2008, *Phys. Rev. Lett.*, 100, 181301